International Core Journal of Engineering Volume 7 Issue 7, 2021
ISSN: 2414-1895 DOI: 10.6919/ICJE.202107_7(7).0049

Structural Analysis of Key Components of Plate Type Solar Cell Module Laminator

Jiahui Zhu[1,2,3], Lei Shi[1,2,3,*], Kun Zhang[1,2,3], Shuzhen Li[1,2,3], Lidong Chen[1,2,3]

[1]College of Mechanical and Electronic Engineering, Hebei Normal University of Science and Technology, Qinhuangdao 066600, China;

[2]Hebei Technology Innovation Center of Photovoltaic Module Manufacturing Equipment, Qinhuangdao 066600, China;

[3]Hebei Engineering Research Center of PV Module Encapsulating and Measuring Equipment, Qinhuangdao 066600, China.

*xnshilei@126.com

Abstract

The three-dimensional model of the laminated plate solar cell component is established by three-dimensional software, and the finite element analysis software ANSYS Workbench is used to analyze the key components of the laminated plate and the heating plate of the laminated plate. The analysis results show that the deformation of the bottom surface of the laminated plate is less than 3.7012×10^{-9} mm and the deformation is uniform, indicating that the force exerted by the electric cylinder on the battery component is balanced. In the heating process, the maximum deformation of heating plate edge is 7.1256×10^{-7} mm, and the deformation is small, which does not affect the pressure effect.

Keywords

Plate Solar Cell Laminator; Static Analysis; Thermal-structural Analysis.

1. Introduction

The plate-type solar cell component laminate press exerts pressure on the solar cell component by pushing the laminate on the top of the electric cylinder. In the process of applying pressure, the force balance of the solar cell component should be ensured, and the requirement for the laminate is relatively high. The distribution of surface temperature and the stability of the structure of the heating plate affect the yield of solar cell components in the process of lamination. It is necessary to carry out thermal coupling analysis of the heating plate structure to analyze the distribution of surface temperature and the stability of the structure.

In this paper, three-dimensional software is used to establish the three-dimensional model of the plate-type solar laminated machine, and the finite element analysis software ANSYS Workbench is used to carry out the static analysis and the thermal-mechanical coupling analysis of the heating plate of the plate solar cell component laminated machine. Through the static analysis, to ensure that the laminate in the process of pressure uniform. The thermodynamic analysis of the heating plate was carried out to determine the rationality of the heating plate structure, so as to improve the heating uniformity of the component and reduce the warpage and the laminated bubbles of the component.

ISSN: 2414-1895 DOI: 10.6919/ICJE.202107_7(7).0049

2. Prototype model of plate press

The prototype model of the plate-type laminating machine is shown in Figure 1, which is mainly composed of five parts: supporting device, driving device, laminating device, oil conveying device for the output and input of heat conducting oil, and vacuum pumping device. The heating plate adopts Q235 carbon structural steel plate. The plate-type laminator is driven by an electric cylinder, and the laminating plate directly applies pressure on the silica gel plate to laminate the battery components.

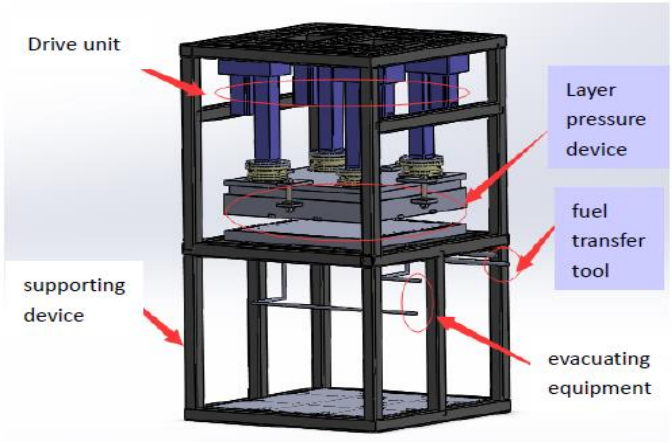

Fig. 1 Three-dimensional model of laminator

3. Mechanics analysis theory

3.1 Static analysis theory

Static analysis is to calculate the effect of the structure under the action of fixed load. It can not only solve the displacement, stress and strain problems caused by external force, but also solve the problems that inertia and damping have relatively small influence on the structure. Static analysis equation [1-2]:

$$[K]\{\chi\} = [F] \tag{1}$$

In the formula, [K] denotes the stiffness matrix, {x} represents the displacement vector, [F] Represents static load.

3.2 Thermal analysis theory

Heat conduction refers to the internal energy exchange caused by the temperature gradient of the object itself [3]. Energy moves from high temperature to relatively low temperature through intermolecular movement. The law of heat conductivity is Fourier law:

$$q = \text{-k}A\frac{dT}{\text{dN}} \tag{2}$$

In the formula, q represents the cut-off heat conductivity, k represents the thermal conductivity of the medium, A represents the cross-sectional area of the medium, and $\frac{\text{dT}}{\text{dN}}$ represents the temperature gradient [4]. When the moving fluid contacts with other objects, as long as there is a temperature difference between the two objects, there will be heat conduction between them. The total heat conduction rate can be described by Newton's cooling equation as:

$$q = hA\ (T_s - T_f) \tag{3}$$

In the formula, h represents the heat transfer coefficient, represents the surface temperature, and represents the temperature of the flow fluid [5].

The amount of energy emitted by the surface can be determined by the following equation:

$$q'' = \varepsilon\sigma T_s^4 \tag{4}$$

ISSN: 2414-1895 DOI: 10.6919/ICJE.202107_7(7).0049

In the formula, q'' represents the heat flow rate per unit area on the surface, ε represents the surface emissivity $0 < \varepsilon < 1$, σ and is Stephen = Boltzmann constant, about 5.67×10^{-8} W / m^2·K^4.

4. Statics analysis of laminated plate of plate type press

4.1 Laminated plate structure

The electric cylinder is used as the driving device in the plate type laminating machine to drive the laminating plate to move up and down. In order to analyze the deformation of the lower surface of the laminating plate under pressure, four electric cylinders are distributed in the position shown in Figure 2.

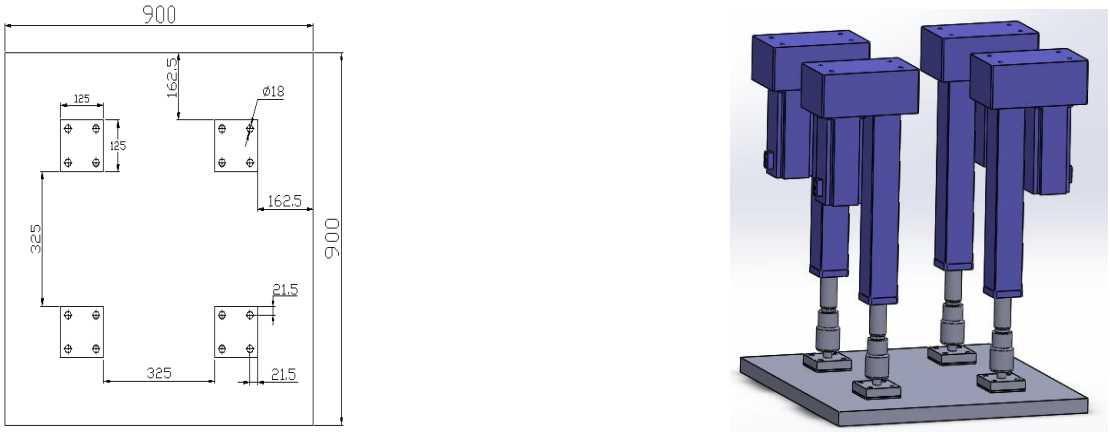

(a) Plan view of laminate (b) Three-dimensional model of laminate and electric cylinder

Fig. 2 Laminate structure

4.2 Static Analysis of Laminates

4.2.1 Definition of material properties and meshing of laminates

The structural property of laminates is defined as Q235, and its characteristic parameters are shown in table 1. The default meshing method in ANSYS module is used to mesh the laminate. The number of nodes in the structure is 7840, and the number of elements is 4384. The grid division is shown in Figure 3.

Table 1. Q235 Performance parameters

attribute types	parameter
elastic modulus(N/m^2)	2.12×10^{11}
poisson ratio	0.288
mass density(kg/m^3)	7.86×10^3

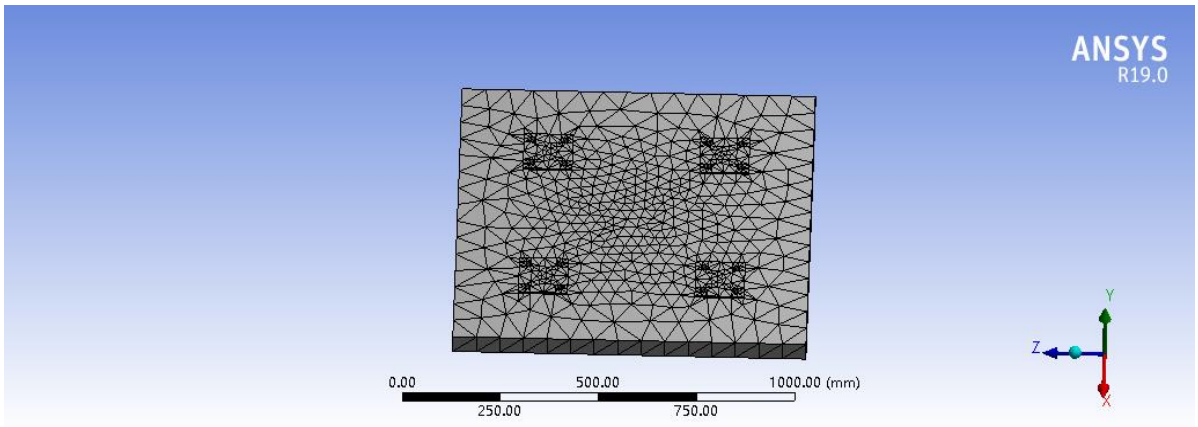

Fig. 3 Mesh division

ISSN: 2414-1895 DOI: 10.6919/ICJE.202107_7(7).0049

4.2.2 Boundary and load

The lower surface is taken as the support surface, and the four surfaces contacted by the upper surface and the rotating joint are taken as the stress surface. When the maximum pressure is applied on each stress surface, it can reach 22000 N (the positions of B, C, D and E should bear the pressure of 22000 N). Considering the gravity of the laminate, the gravity acceleration is set to 9.8066 m / s^2, as shown in Figure 4.

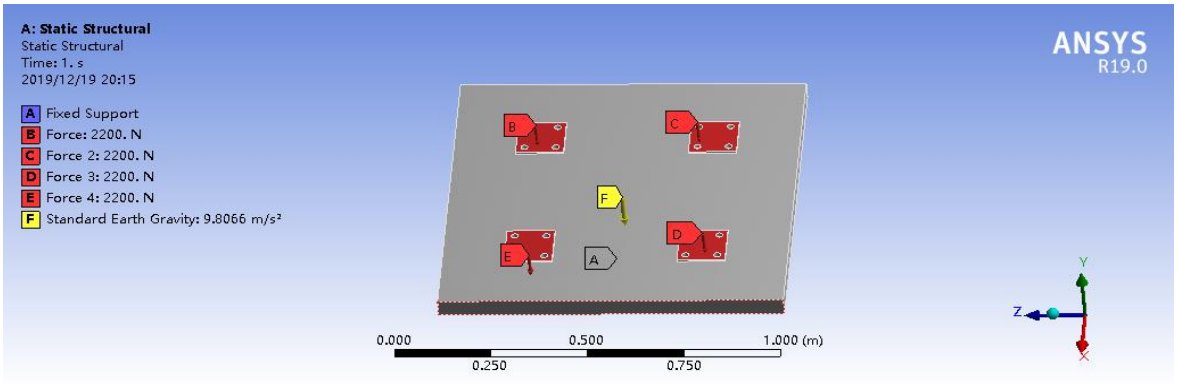

Fig. 4 Boundary conditions

4.2.3 Results of static analysis

The displacement nephogram is obtained. Figure 5 (a) is the displacement nephogram of the stress surface of the laminate, and the maximum deformation is 3.311×10^{-8} m, which does not affect the laminate process. As shown in Figure 5 (b), the displacement nephogram on the back of the stress surface is shown. The deformation variable is less than 3.7012×10^{-9} m, and there is almost no deformation. The results show that during the lamination process, the back of the laminate is plane, and the flatness of the solar cell component can be guaranteed if the force of the battery component is uniform.

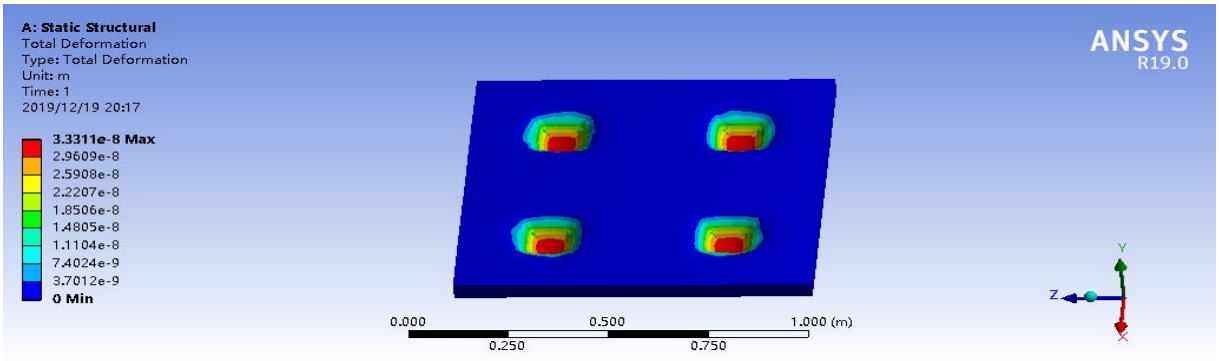

(a) Displacement cloud map (forced surface)

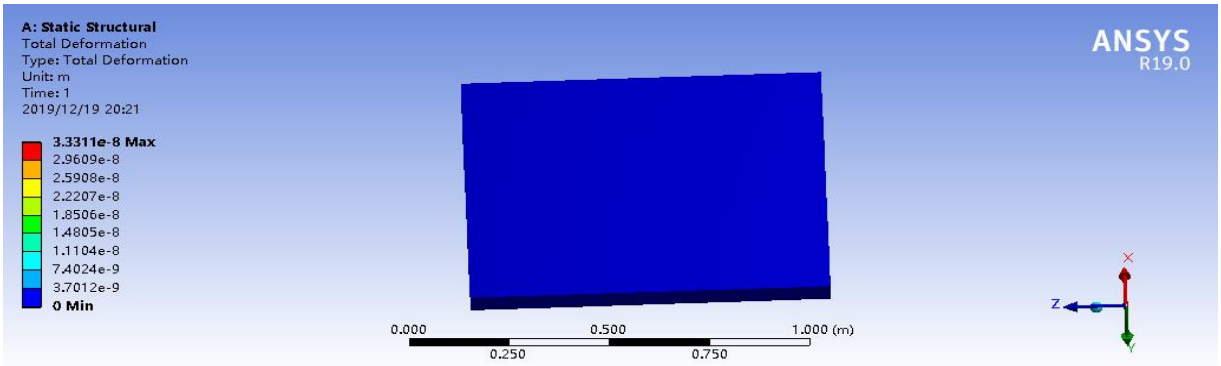

(b) Displacement cloud image (back)

Fig. 5 Displacement cloud diagram

ISSN: 2414-1895 DOI: 10.6919/ICJE.202107_7(7).0049

Figure 6 shows the equivalent stress nephogram. The maximum stress is 1.3814×10^5 Pa, which is far less than the yield strength of the selected material Q235. The reasonable design of the laminate structure can be determined from the displacement nephogram and the equivalent stress nephogram.

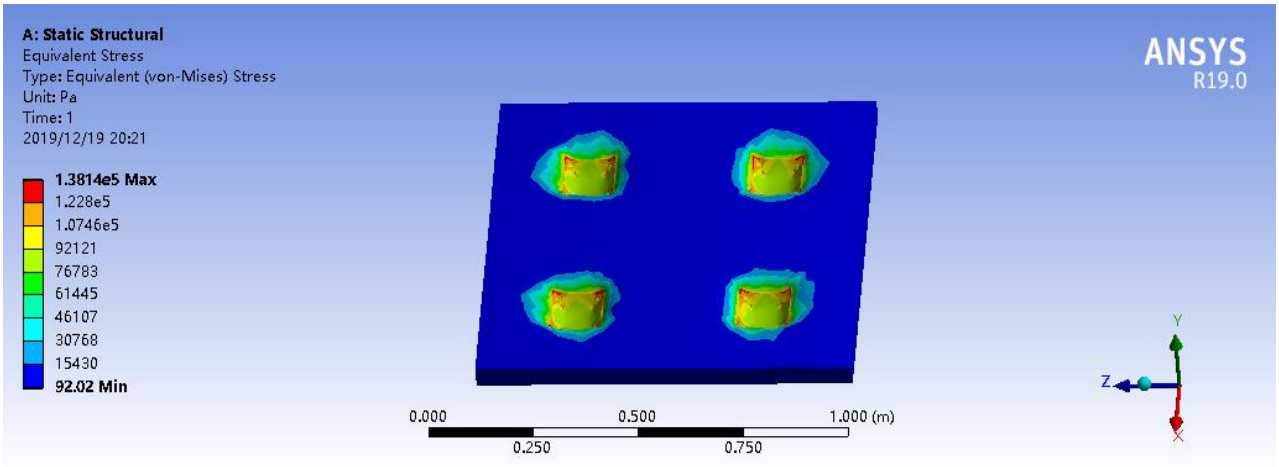

Fig. 6 Equivalent stress cloud diagram

5. Thermal-mechanical coupling analysis of heating plate

5.1 Heating plate structure

The heating plate material is defined as Q235, and some material properties have been given in Table 1. The thermal conductivity of the material is 43W/ (m °C), and the specific heat coefficient is 0.44 kj / (kg / °C). The structure size of the heating plate of the press is 1000 mm×1000 mm×60 mm, and the serpentine pipeline of the heat conducting oil is arranged inside, and the diameter of the pipeline is Φ30. Seven vacuum holes are set at the two ends of the upper surface, and one vacuum hole is set at the middle part of the two ends of the lower surface. The upper and lower vacuum holes are connected through the Φ24 mm through holes at both ends. The upper surface holes are connected with the inner cavity between the upper and lower boxes, and the lower surface holes are connected with the vacuum pump. The Φ24 mm through holes are sealed at both ends when they are working. There are four temperature sensor connecting holes on the lower surface. Figure 7 is the two-dimensional structure of the heating plate, and Figure 8 is the internal structure of the three-dimensional model.

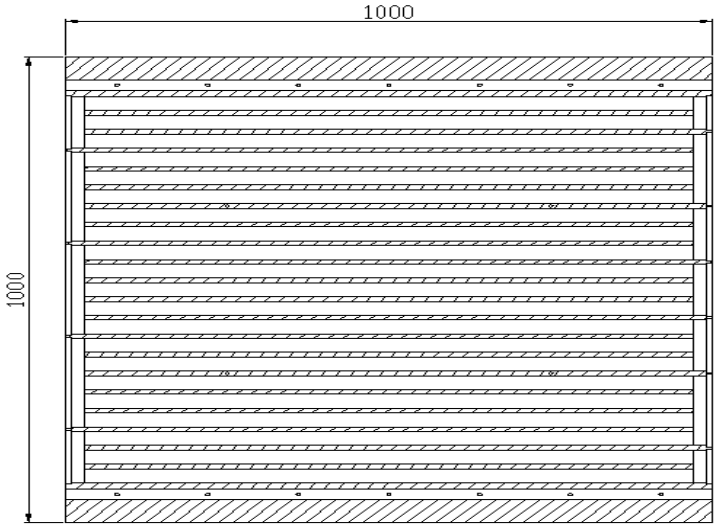

Fig. 7 Two-dimensional structure of the heating plate

ISSN: 2414-1895 DOI: 10.6919/ICJE.202107_7(7).0049

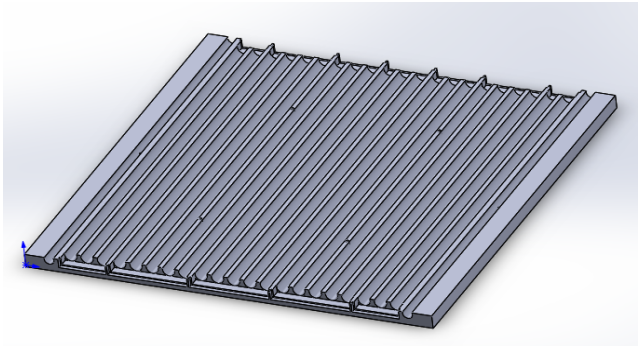

Fig. 8 Three-dimensional structure of the heating plate

Heating plate heat conducting oil adopts shell SD-320 heat conducting oil, material properties as shown in table 2.

Table 2. SD-320 heat conducting oil parameter table

model	pour point (℃)	specific gravity (g/cm^3)	Motion viscosity at 40°C (cSt)	flash point (℃)	ignition point (℃)	solidifying point (℃)
SD-320	-30	320	32.62	226	206	-30

5.2 Thermal-mechanical coupling analysis of heating plate

5.2.1 Physical model import and mesh generation

The three-dimensional model of the heating plate drawn by Solidworks is imported into ANSYS Workbench. The thermal steady-state analysis module is selected, the material properties are defined, and the heating plate structure is meshed. Due to the large size of the heating plate, the complex internal heat conduction oil pipeline and the complex distribution of vacuum holes and sensor installation holes, the heating plate structure is meshed by default state. There are 133148 nodes and 76382 units, as shown in Figure 9.

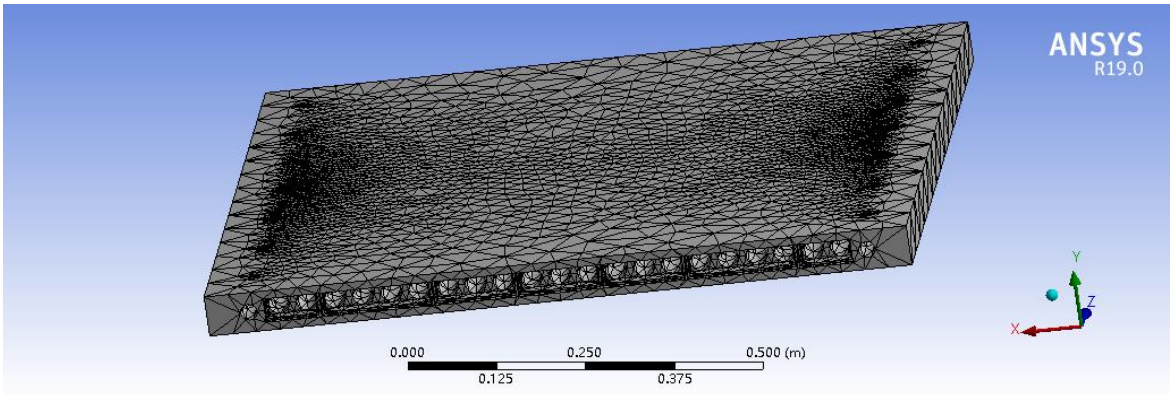

Fig. 9 Heating plate grid division

5.2.2 Boundary and load

During the lamination process of solar cell components, the Forster POE film is used, and the preset temperature is 150 ℃, that is, the temperature load on the heat conduction oil pipeline is 150 ℃. Convective heat transfer coefficient was applied on the surface of heat conduction oil circuit at 461.36 W / m2 ℃. The convective heat transfer coefficient is 5W / m^2 ℃. The radiation coefficient is 0.79. The heating plate surface is set to an adiabatic surface. The boundary conditions imposed by the heating plate are shown in Figure 10.

ISSN: 2414-1895 DOI: 10.6919/ICJE.202107_7(7).0049

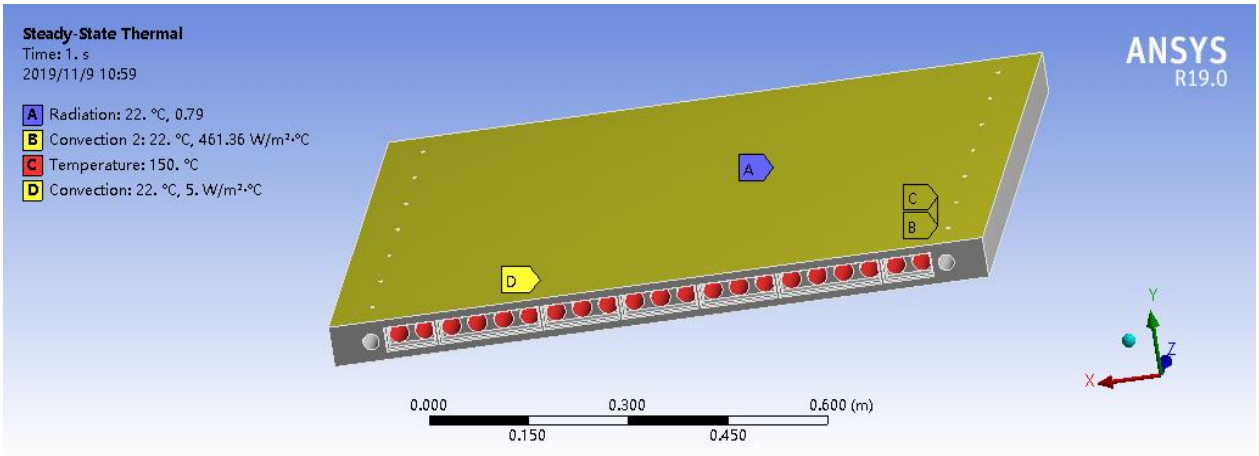

Fig. 10 Boundary conditions

5.2.3 Steady-state thermal analysis

Figure 11 is the temperature distribution map of the heating plate. It can be clearly seen that the highest temperature value appears in the internal of the serpentine pipeline, and its value is 150.19 °C. The minimum temperature appears around the heating plate, which is 145.35 °C. The temperature in the layer pressure interval on the surface of the heating plate was 149.11°C–149.65°C, which was sufficient to make POE melt, proving the rationality of the heating plate structure.

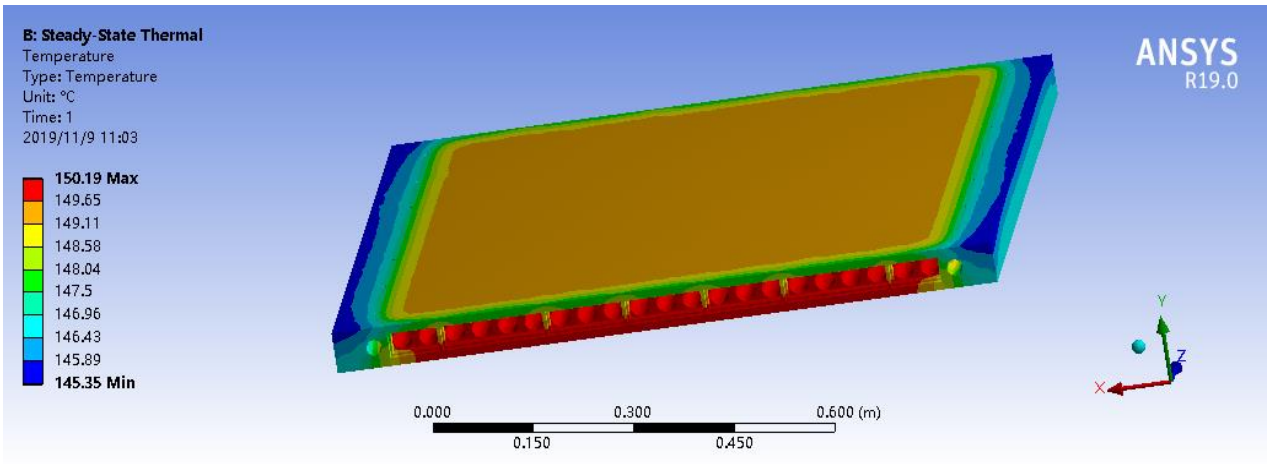

Fig. 11 Temperature distribution of the heating plate

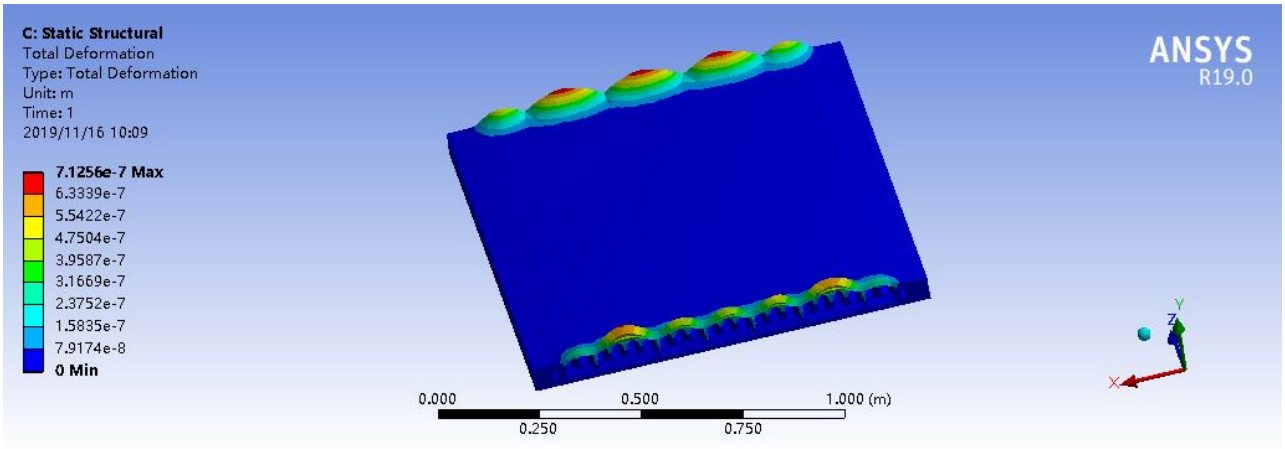

Fig. 12 Cloud diagram of heating plate displacement

ISSN: 2414-1895 DOI: 10.6919/ICJE.202107_7(7).0049

5.2.4 Thermal-mechanical coupling analysis of heating plate

Based on the thermodynamic analysis of the heating plate, the thermal-mechanical coupling is studied. The heating plate is meshed by default, and the bottom of the heating plate is selected as the support surface. A pressure of atmospheric pressure is applied on the upper surface by applying its own gravity load. The displacement nephogram shown in Figure 12 is obtained. The maximum displacement is 7.1256×10^{-7} m, which occurs at both ends of the serpentine pipeline. Within the allowable error range, the rationality of the heating plate structure design is proved.

6. Conclusion

In this paper, the main structure of the laminating part of the plate press is drawn by using Solidworks 3D modeling software. The thermal analysis and static analysis of the key components of the plate laminating machine were carried out. The analysis results show that the deformation of the bottom surface of the laminate is small and uniform during the lamination process, indicating that the force exerted by the battery components is balanced during the force application of the electric cylinder. In the heating process, the edge deformation of the heating plate is small, which does not affect the layer pressure effect, and the structure design of the heating plate is reasonable.

Acknowledgments

This work is supported by Major achievements transformation project in Hebei Province, Project number: 19014312Z, and Research project on teaching reform in Hebei Normal University of science and technology in 2019, Project number: JYYB201902.

References

[1] Gao Changyin, Li Wanquan, Liu Li, etc. ANSYS Workbench 14.5 Modeling and Simulation [M]. Beijing, Electronic Industry Press, 2014.

[2] Tian Keqing, Zhang Kun, Wu Yu, etc., modeling and simulation analysis of KB20 self-propelled curbstone sliding machine frame [J]. Science and technology innovation report, 2018,15 (33): 83-85.

[3] Sun Jianqiang. The experimental analysis of buckling and thermal fatigue of nano-scale thin films under force-thermal coupling field [D]. Tianjin University, 2008.

[4] Long chengshu. Paddy heat pump drying process and key components design [D]. Central South University of Forestry and Technology, 2014.

[5] Xu. Numerical simulation and performance analysis of concrete based on material meso-structure [D]. Zhejiang University, 2008.